

## Article

# Mathematical Model of Basal Sprout Production in Vector-Borne Tree Disease

Kelly Ruth Buch <sup>1,2,\*</sup>  and Nina H. Fefferman <sup>2,3,4</sup> <sup>1</sup> Department of Mathematics and Statistics, Austin Peay State University, Clarksville, TN 37044, USA<sup>2</sup> Department of Mathematics, University of Tennessee, Knoxville, TN 37996, USA<sup>3</sup> Department of Ecology and Evolutionary Biology, University of Tennessee, Knoxville, TN 37996, USA<sup>4</sup> National Institute for Mathematical and Biological Synthesis, Knoxville, TN 37996, USA

\* Correspondence: buchk@apsu.edu

**Abstract:** Some tree species respond to disease by producing basal sprouts from the base and root system of a dying tree, which can alter disease dynamics by altering demography. In the case of many lethal, airborne tree diseases, the production of basal sprouts can be a key contributor to population resurgence post-epidemic, but the effect in lethal, vector-borne tree diseases has not yet been studied. To determine the role of basal sprout production and secondary infection via the root system of infected parent trees in lethal, vector-borne tree diseases, we develop a stage-structured SI-X mathematical model and use laurel wilt, a vector-borne tree disease in which infected trees provide suitable material for vector reproduction, as our model system. The mathematical model shows that the production and secondary infection of basal sprouts do not affect the short-term dynamics of laurel wilt but profoundly alter the long-term dynamics of the laurel wilt epidemic. In particular, in the absence of basal sprout infection, basal sprout production yields a larger host population after disease establishment, but as secondary infection increases, the utility of basal sprouts to maintain the host population decreases. Results suggest management strategies for lethal, vector-borne diseases should depend on the ratio of the basal sprout production rate to the secondary infection rate.



**Citation:** Buch, K.R.; Fefferman, N.H. Mathematical Model of Basal Sprout Production in Vector-Borne Tree Disease. *Forests* **2023**, *14*, 349. <https://doi.org/10.3390/f14020349>

Academic Editors: Yueh-Hsin Lo and Ester González-de-Andrés

Received: 29 December 2022

Revised: 1 February 2023

Accepted: 2 February 2023

Published: 9 February 2023



**Copyright:** © 2023 by the authors. Licensee MDPI, Basel, Switzerland. This article is an open access article distributed under the terms and conditions of the Creative Commons Attribution (CC BY) license (<https://creativecommons.org/licenses/by/4.0/>).

## 1. Introduction

Since 1850, sixteen nonnative forest pathogens that kill or damage trees have been introduced to the United States, and at least five of these pathogens are vectored by insects [1]. Introduced forest pathogens have devastating effects on forest ecosystems, affecting both the trees themselves and other plant and animal species that depend on the affected tree species. This results in an estimated loss of \$2.1 billion in forest products per year in the United States [2]. It is important to develop management strategies quickly after the introduction of a new forest pathogen into an ecosystem to either eradicate it or mitigate its effects. An understanding of the role of specific factors that influence disease dynamics can assist in developing better management strategies for current diseases and future disease introductions.

Below-ground basal sprouting and root suckering (stems which sprout from the root system of an existing tree) are commonly observed forms of vegetative growth in angiosperms and are often induced when damage (e.g., fire, logging, disease) kills the main stem of a tree but the root system remains intact [3]. Demographic shifts (increased population size and altered stage structure) following disease-induced production of basal sprouts may be both ecologically and epidemiologically important. Of ecological importance, the production of basal sprouts by damaged trees can maintain (or increase) host population size following a disturbance [4]. Because widespread mortality of trees can inhibit seed production, basal sprouting by damaged trees represents the main path for

host reproduction especially if the reliance on, or longevity of, seed banking is limited [5]. Of epidemiological importance, replacement of mature stems with basal sprouts may cause a demographic shift toward smaller stemmed trees. Pre-disturbance changes in the demography of the tree host can affect disease dynamics [6]. Similarly, basal sprouts produced in response to pest attack and/or pathogen infection in a vector-borne tree disease system may then affect the ecological and epidemiological dynamics of the disease through changes in the overall demography of the host population [3].

In vector-borne disease systems, the specific influence of basal sprout production on disease dynamics is relatively unknown, and existing mathematical models for vector-borne diseases are insufficient to determine it. Pine wilt is a vector-borne disease caused by a parasitic nematode (*Bursaphelengus xylophilus*) and transmitted by pine sawyer beetles (*Monochamus* spp.) [7]. This vector-borne disease kills pine trees (*Pinus* spp.) and has been modeled extensively [8,9]. However, the infected gymnosperms do not respond to infection by producing basal sprouts. As such, production of basal sprouts is not included in models of pine wilt. Dutch elm disease, which is caused by *Ophiostoma* spp. and vectored by the elm bark beetle (*Scolytus multistriatus*), has caused widespread mortality of elm (*Ulmus* spp.) trees across the globe, and some (but not all) species of elm respond to infection by producing basal sprouts [10]. However, the vector that transmits Dutch elm disease is only attracted to mature trees, leading to disease cycles as young trees mature. An untested hypothesis suggested that basal sprout production could account for some of difference between disease dynamics in some species [11,12]. Dutch elm disease models that included the growth of root suckers predicted either an endemic disease state or a disease-free state, depending on parameter values, but the models do not differentiate saplings from basal sprouts; accordingly, the specific role of basal sprouting could not be investigated independently using this model [13,14]. Thus, the specific role of basal sprouts in lethal, vector-borne disease systems is relatively unknown, despite the potential importance of this trait on disease dynamics and host population outcomes.

In producing the first model to investigate the role of basal sprouts in a vector-borne disease system, we focus on laurel wilt as our case study. Laurel wilt is a lethal, vascular tree disease, caused by the fungus *Raffaelea lauricola* and vectored by the redbay ambrosia beetle (*Xyleborus glabratus*) [15]. The insect-pathogen complex is not considered a pest in its native range of Asia, but the fungus is pathogenic to trees within the laurel family (Lauraceae) in its introduced range in North America [16]. Upon infection, the fungus moves systematically through the xylem of the host and induces a host response that leads to crown dieback, leaf wilting, and sapwood discoloration [15]. Disease kills the main stem of trees within weeks (at most two months), inhibiting seed production and inducing the production of basal sprouts from the still-living root system [17].

The redbay ambrosia beetle is a wood-boring beetle that has a symbiotic relationship with the pathogenic fungus and requires dead and dying laurel trees for successful brood production. Female ambrosia beetles bore into the woody material of dying host trees (male ambrosia beetles are flightless and do not attack trees), creating small tunnels called galleries in which they cultivate their symbiotic fungus to feed their larvae. In contrast to other species of ambrosia beetle, redbay ambrosia beetles will also bore into healthy host trees with no signs of distress, with a preference for large-stemmed trees. Boring attempts into healthy trees do not yield successful brood production and are abandoned; however, enough fungal pathogen is transferred to infect the tree with laurel wilt. This contact is the primary transmission route for laurel wilt [15]. As they start to die, infected trees provide suitable host material for redbay ambrosia brood production, but tree material is eventually degraded by excessive gallery production.

Redbay (*Persea borbonia* (L.) Sprengel) and sassafras (*Sassafras albidum* (Nutt.) Nees) are two ecologically important members of the laurel family and are susceptible to laurel wilt. Redbay is an evergreen tree with natural range covering the southeastern coastal plain and Florida, and sassafras is a deciduous tree that spans the majority of Eastern United States [18,19]. Laurel wilt is known to kill greater than 90% of large redbay stems in

2–3 years [20]. About half the range of sassafras occurs in regions with winter temperatures consistent with redbay ambrosia beetle cold tolerance, but as of now, laurel wilt is present in only a small portion of the range of sassafras [21]. Accordingly, studies of laurel wilt infection in sassafras over long time scales have not been done yet, and little is known about the disease dynamics in this new host range.

Newly infected redbay and sassafras trees can respond to laurel wilt infection by producing healthy basal sprouts or epicormic shoots [20]. These basal sprouts are not infected but can become infected via direct contact with the root system of the infected parent tree, representing the secondary transmission route for laurel wilt. Because redbay ambrosia beetles rarely attack small diameter stems, infection of basal sprouts via secondary transmission can occur more quickly than infection via primary transmission; a sprout must mature sufficiently to be attractive enough for primary transmission to occur [16]. The degree to which trees produce basal sprouts in response to infection and the rate of secondary transmission via connected root systems are both species dependent, so these differences could lead to qualitatively different disease dynamics in different species of susceptible host populations.

Our aim is to investigate, through mathematical modeling, the ecological and epidemiological dynamics of laurel wilt as a case study by which to provide broader insight into the processes of all lethal, vector-borne tree diseases. We build and analyze a model to determine the potential impact of basal sprout production and infection on stand-level disease progression and survivorship. Understanding the role of basal sprouts in epidemic progression will provide insight into how to best manage for lethal, vector-borne diseases and illuminate differences to expect in host species that respond with basal sprout production at varying intensities. Mathematical models can isolate the effects of specific components of tree disease dynamics in ways that cannot be manipulated for empirical study directly (i.e., limiting physical or temporal constraints); therefore, as introductions of new tree diseases threaten arboreal biodiversity across the globe, increasing the set of appropriate mathematical models available as tools to support management and mitigate long-term consequences will be critical.

## 2. Materials and Methods

We develop a mathematical model for laurel wilt using ordinary differential equations following the SI-X framework [22] (with X representing vector population as a proxy for total inoculum) and incorporate discrete host-stage structure. Host trees are considered infected if they harbor the fungal pathogen (and thus provide suitable host material for vector brood production) and susceptible otherwise. We separate susceptible and infected trees into several discrete classes representing host size, consistent with size classes often reported in data collection [20]. In particular, we separate susceptible trees into  $P_S(t)$ ,  $M_S(t)$ ,  $L_S(t)$ , and  $B_S(t)$  representing the number of susceptible saplings, medium trees, large trees, and basal sprouts, respectively, in each size class and then separate infected trees into  $P_I(t)$ ,  $M_I(t)$ ,  $L_I(t)$ , and  $B_I(t)$  representing the volume of suitable host material (rather than the number of trees) for vector brood production provided by saplings, medium trees, large trees, and basal sprouts respectively. The host seed bank is denoted by  $D(t)$  and is considered neither susceptible nor infected. The final class,  $X(t)$ , represents the number of female adult vectors. Due to the obligate nature of the vector-pathogen system [18], all

vectors are assumed to carry the pathogen. The differential equations of the model are given by

$$\begin{aligned}
 \frac{dD}{dt} &= r_M M_S + r_L L_S - \gamma D - \mu_D D \\
 \frac{dP_S}{dt} &= \gamma D - g_P P_S - \mu_P P_S - \beta_P P_S X \\
 \frac{dM_S}{dt} &= g_P P_S + g_B B_S - g_M M_S - \mu_M M_S - \beta_M M_S X \\
 \frac{dL_S}{dt} &= g_M M_S - \mu_L L_S - \beta_L L_S X \\
 \frac{dB_S}{dt} &= \rho_M \frac{M_I}{v_M} + \rho_L \frac{L_I}{v_L} - (\sigma + g_B + \mu_B) B_S \\
 \frac{dP_I}{dt} &= v_P \beta_P P_S X - \delta_P P_I X \\
 \frac{dM_I}{dt} &= v_M \beta_M M_S X - \delta_M M_I X \\
 \frac{dL_I}{dt} &= v_L \beta_L L_S X - \delta_L L_I X \\
 \frac{dB_I}{dt} &= v_B \sigma B_S - \delta_B B_I X \\
 \frac{dX}{dt} &= \omega X \left( 1 - \frac{v_0 X}{P_I + M_I + L_I + B_I} \right).
 \end{aligned} \tag{1}$$

A flow diagram representing the movement between compartments of the model is shown in Figure 1.

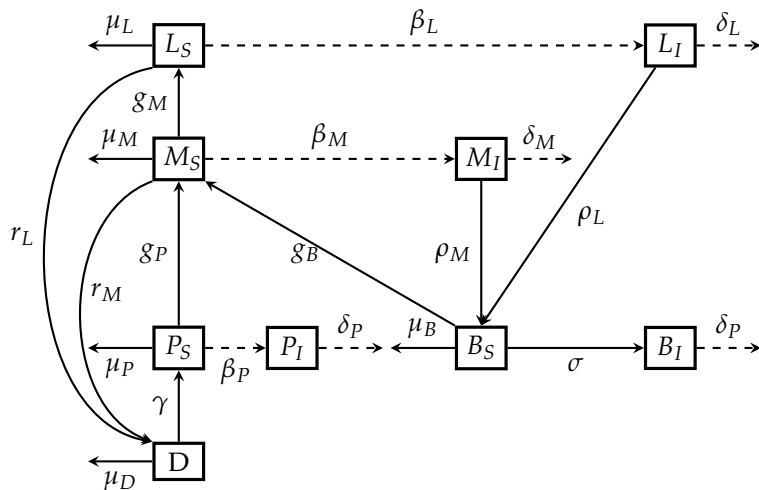


**Figure 1.** Flow diagram for Model (1). Solid lines represent flow between host size and infection classes that occurs independent of vector population size, and dashed lines represent flow between host size and infection classes that is dependent on vector population size. Lines directed upward represent maturation between host stages, curves directed downward represent host reproduction (seed and basal sprout production), and lines with lateral direction represent death, infection, or degradation of host trees.

### 2.1. Host Dynamics

Susceptible host dynamics include seed germination, maturation, natural mortality, and seed production. Saplings mature to medium susceptible trees at rate  $g_P$ , and susceptible medium trees mature to susceptible large trees at rate  $g_M$ . Similarly, susceptible basal sprouts mature to medium trees at rate  $g_B$ . Saplings, medium trees, large trees, and basal sprouts suffer natural mortality at rates  $\mu_P, \mu_M, \mu_L$ , and  $\mu_B$ , respectively. Both susceptible

medium and large trees contribute to the seed pool at rates  $r_M$  and  $r_L$ , respectively. Seeds either deteriorate at rate  $\mu_D$  or germinate into susceptible saplings at rate  $\gamma$ . Neither redbay nor sassafras maintain long-term seed pools (redbay seed are not viable after two years [17] and sassafras seeds can remain viable up to 5–6 years, but the germinative capacity after 5 years is low [23]), so we only consider appropriately large values for  $\mu_D$ .

Infected host classes do not grow or contribute to the seed pool, but infected medium and large trees respond to laurel wilt infection by producing susceptible basal sprouts at rates  $\rho_M$  and  $\rho_L$ , respectively. This production is scaled by  $v_M$  and  $v_L$ , the volume of medium and large trees, respectively. Infected host material of all classes is degraded through the use of infected trees by vector for brood production, rendering it unsuitable for future beetle brood production. This degradation is represented by the outgoing terms  $\delta_Z Z_I X$ , where  $Z$  is a place holder for the volumes of infected saplings, medium trees, large trees, and basal sprouts and  $\delta_Z$  is the size-specific degradation rate.

## 2.2. Vector Dynamics

In laurel wilt and other vector-borne tree diseases, the vector requires infected host material for successful reproduction, and vector populations decline as disease prevalence declines [24,25]. Accordingly, we assume the vector population growth depends on both the current beetle population size and the volume of infected trees. We capture these assumptions through logistic growth with a nonconstant carrying capacity dependent on the total amount of infected host volume. We define the nonconstant carrying capacity,  $K$ , as the ratio of the total available volume of infected tree and the volume of infected host required for each beetle gallery ( $v_0$ ), i.e.,

$$K = \frac{P_I + M_I + L_I + B_I}{v_0}.$$

For simplicity, we assume that beetles reproduce equally efficiently in any equivalent volume of infected material, regardless of the size of tree from which that material originated (despite some empirical evidence suggesting otherwise [25]; extensions of this work to relax this assumption are planned for the future; preliminary sensitivity explorations suggest that the outcome may be robust across sizes).

## 2.3. Infection Transmission

Transmission of the fungal pathogen occurs via two routes. The primary transmission occurs with contact between vector and susceptible tree at rates  $\beta_Z$ , with incidence terms  $\beta_Z Z_S X$ , where  $Z$  is a place holder for the volumes of infected saplings, medium trees, and large trees. This transmission route represents the abandonment of unsuccessful boring attempts into healthy trees. We take  $\beta_P < \beta_M < \beta_L$  to account for the vector's preference for large stems. Incidence terms are scaled by the tree's volume,  $v_Z$ , producing a positive term  $v_Z \beta_Z Z_S X$  into each of the differential equations for the volume of infected saplings, medium trees, and large trees. Secondary transmission is the direct transmission of pathogen from infected medium and large trees to susceptible basal sprouts and occurs at rate  $\sigma$ . Susceptible basal sprouts are scaled by  $v_B$ , the volume of a basal sprout, and transferred into the infected basal sprout class. This secondary transmission occurs without vector involvement because basal sprouts are physically attached to an infected tree via the root system.

## 2.4. Model Parameterization and Analysis

We consider numerical approximations of solutions to the differential equations in and equilibria of Model (1) using a biologically feasible range of parameter values. The default value for each parameter is listed in Table 1. When possible, values are estimated from data. In absence of data, values were assumed and then varied to test the sensitivity of the model to the assumption. See Appendix A for further detail on chosen parameter values.

To reduce the degrees of freedom among the parameters and to maintain ecologically relevant orderings of parameters even when exact values are not known, we assume relationships among stage-specific host parameters. We assume the rate of seed production for medium trees is 90% that of large trees, the medium tree and basal sprout maturation rates are equivalent and are 40% that for large trees, and the natural mortality rates of saplings and medium trees are twice and thrice that of large trees, respectively. We further assume that size specific primary transmission rates increase with tree size such that the rates for sapling and medium trees are 1% and 25% that of large trees, respectively. As a gross estimate for volume of trees, we assume that infected saplings and basal sprouts contribute equivalent volume and that medium and large trees contribute twice and four times as much, respectively. Due to a lack of differentiating information, we assume that basal sprout production is equivalent for large and medium trees ( $\rho := \rho_M = \rho_L$ ) and host degradation rate is equivalent for all stems ( $\delta := \delta_B = \delta_P = \delta_M = \delta_L$ ). In all cases, the scaling values are chosen arbitrarily to yield a parameter regime with the desired parameter inequalities.

**Table 1.** Summary of stage specific parameters and their default values used in Model (1). See Appendix A for calculations and references. Values are presented with one significant digit.

Description	Units	Symbol	Default Value
Seed production rate	year <sup>-1</sup>	$r_L$	0.3
		$r_M$	0.9 $r_L$
Seed germination rate	year <sup>-1</sup>	$\gamma$	0.1
Maturation rate	year <sup>-1</sup>	$g_P$	0.08
		$g_B$	$g_P$
		$g_M$	0.4 $g_P$
Natural mortality rate	year <sup>-1</sup>	$\mu_D$	0.3
		$\mu_L$	0.01
		$\mu_M$	2 $\mu_L$
		$\mu_P$	3 $\mu_L$
		$\mu_B$	0.001
Primary transmission rate	year <sup>-1</sup> beetle <sup>-1</sup>	$\beta_L$	0.02
		$\beta_M$	0.3 $\beta_L$
		$\beta_P$	0.01 $\beta_L$
Secondary transmission rate	year <sup>-1</sup>	$\sigma$	1
Basal sprout production rate	year <sup>-1</sup>	$\rho_L$	2
		$\rho_M$	$\rho_L$
Volume of host	units <sup>3</sup>	$v_L$	4
		$v_M$	2
		$v_P$	1
		$v_B$	1
Host degradation rate	year <sup>-1</sup> beetle <sup>-1</sup>	$\delta_L$	0.02
		$\delta_M$	$\delta_L$
		$\delta_P$	$\delta_L$
		$\delta_B$	$\delta_L$
Volume of beetle gallery	units <sup>3</sup>	$v_0$	0.3
Vector per capita reproductive rate	year <sup>-1</sup>	$\omega$	8

When parameters are changed from the default, we define low and high values as 50% and 200% of the default value, respectively. When considering a range of values of certain parameters, we use Latin hypercube sampling and sample values between the low and high value for each parameter. Related parameters are varied proportionally, and when a parameter is not varied, its default value is used. (Note: the set of parameters we assumed to be related were chosen such that independent variations would not affect the qualitative outcomes of the modeled dynamics, only the rapidity and magnitude of the outcomes).

### 3. Results

We investigate both the short-term (transient) and long-term (asymptotic) dynamics of the mathematical model, focusing on the effects of the rates of basal sprout production ( $\rho$ ) and secondary infection ( $\sigma$ ). We first consider the dynamics of the system without basal sprouting ( $\rho = 0$ ). In the absence of basal sprouting (and otherwise at default parameter values), all host populations decline after disease introduction, with the large tree population hitting 80% mortality first after 1.46 and the vector population reaching a peak at 1.56 years (Figure 2, solid line). Within a parameter space of 250 samples varying  $r_Z$ ,  $\gamma$ ,  $g_Z$ ,  $\mu_D$ , and  $\beta_Z$ , trajectories follow similar dynamics, but the timing of crashes and peaks varies. In particular, with varied host growth and transmission parameters, the large tree population reaches 80% mortality between 1.0 and 2.6 years after infection, and the vector population peaks between 1.2 and 2.2 years.

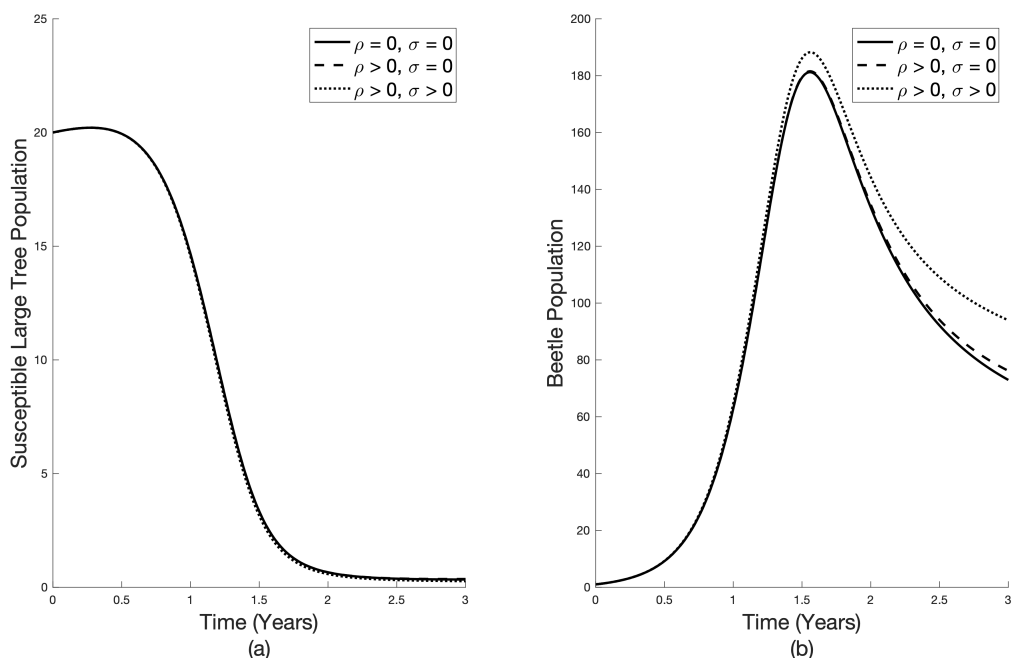


**Figure 2.** Susceptible large tree population and vector population over three years with no basal sprout production (solid line), basal sprout production with no secondary infection (dashed line), and basal sprout production with secondary infection (dotted line). (a) Initial decline of susceptible population is invariant under basal sprout production and infection. (b) The vector population peaks at 1.56 years. The maximum size of the vector population is dependent on basal sprout production and infection, but when the maximum occurs is invariant with respect to basal sprout production and infection. Unless zero, all parameters take the default values.

We then consider low, default, and high rates of basal sprout production ( $\rho$ ) with coupled with no, low, default, and high rates of secondary infection ( $\sigma$ ) for all 250 samples. Throughout this parameter space, the time to 80% mortality changes by at most 0.23 years (with the largest changes occurring when  $\beta$  is smallest). The time of the peak of the vector population is largely unaffected by basal sprouting, with the peak changing by at

most 0.03 years for varied values of  $\rho$  and  $\sigma$ . However, the size of the beetle population at the peak does increase as either  $\rho$  or  $\sigma$  increase. Throughout this parameter space, large values of  $\rho$  and  $\sigma$  yield a peak population size no more than about 25 beetles larger than the peak population size in absence of basal sprouting. Trajectories of the large tree and vector populations at the default parameter values with no basal sprout production, sprout production in absence of secondary infection, and sprout production with secondary infection are given in Figure 2.

Equilibrium analysis of the system shows three biologically feasible equilibria: a vector-and-host extinction equilibrium, a disease-free equilibrium, and an endemic equilibrium. The disease-free equilibrium is a boundary case that only exists when growth and death parameters balance correctly. The endemic and extinction equilibria both exist. The extinction equilibrium is unstable, and numerical simulations suggest the stability of the endemic equilibrium is robust throughout the biologically feasible parameter space (see Appendix B). In particular, the production and secondary infection of basal sprouts do not affect the existence or stability of equilibria.

The production and secondary infection of basal sprouts have profound effects on the size of both host and vector populations at the endemic equilibrium. In the absence of secondary infection ( $\sigma = 0$ ), the production of basal sprouts yields a larger host population at endemic equilibrium. Although the host population can persist without basal sprouting ( $\rho = 0$ ) when seed production and germination are high ( $\gamma$  and  $r_Z$  200% of default), the number of susceptible medium trees at the endemic equilibrium is nearly zero, and thus not biologically feasible when  $\rho = 0$ . In either case, the number of susceptible medium trees at the endemic equilibrium increases approximately linearly as  $\rho$  increases (Figure 3). Other classes of susceptible hosts follow similar trends.

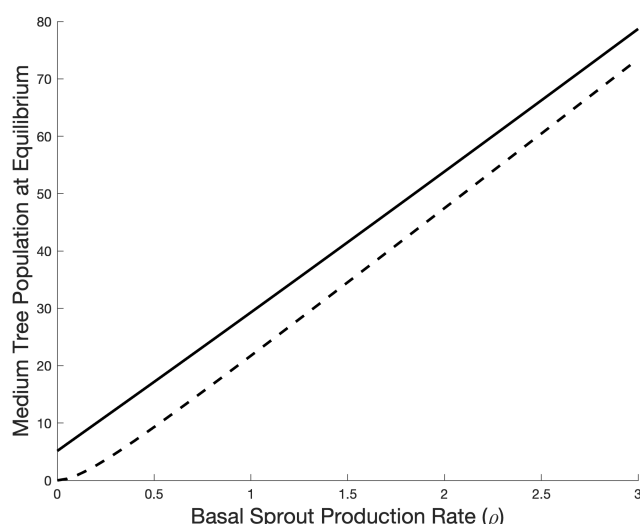


**Figure 3.** Medium tree population size at equilibrium with no secondary infection for low (dashed, 50% of default) and high (solid, 200% of default) seed production and germination. The size of the medium tree population at the endemic equilibrium increases as basal sprout production rate increases when there is no secondary infection in both cases.

In the case of basal sprout production with secondary infection ( $\rho > 0, \sigma > 0$ ), the production of basal sprouts increases the host population compared to that with no production for small rates of basal sprout infection. In particular, when the ratio of basal sprout secondary infection rate to basal sprout production rate is low ( $\frac{\rho}{\sigma} < 10^{-3}$ ), the effect of secondary infection is negligible. Host populations at equilibrium are only slightly smaller than they are with no secondary infection. However, as the rate of basal sprout secondary infection increases relative to the production rate, the utility of basal sprouts decreases and host populations at equilibrium decline significantly (Figure 4). When seed production and germination rates are low, high ratios of basal sprout infection rate to

production rate yield medium tree population sizes at equilibrium near zero (Figure 4a), comparable to the population at equilibrium without basal sprout production ( $\rho = 0$ ). When seed production and germination rates are high, high ratios of basal sprout secondary infection rate to production rate yield medium tree population sizes at equilibrium much larger than zero. However, the population is smaller than that with no basal sprout production (Figure 4b).

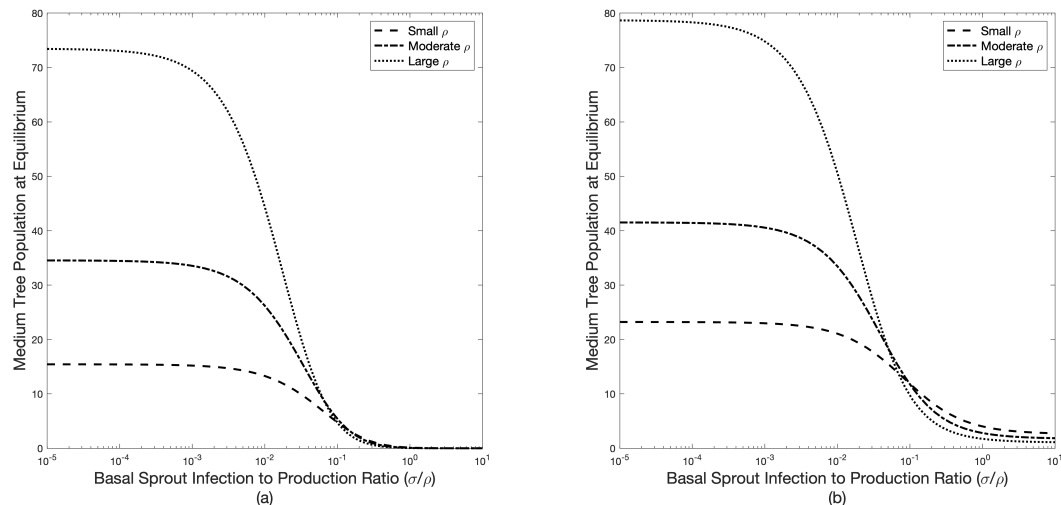


**Figure 4.** Medium tree population at equilibrium size with secondary infection (a) with low values of seed production and germination ( $r$  and  $\gamma$ , 50% of default) and (b) with high values of seed production and germination (200% of default). As basal sprout secondary infection ( $\sigma$ ) increases, the medium tree population at equilibrium declines for low (solid), default (dashed), and high (dot dashed) basal sprout production ( $\rho$ ).

#### 4. Discussion

Our results show that the production and secondary infection of basal sprouts by infected trees in response to disease are unlikely to affect the short-term dynamics of the disease but can profoundly affect the size of host population over longer time scales. Basal sprouts do not affect the initial spread of disease and tree mortality because the time scale of initial disease dynamics is much faster than the time scale of basal sprout production. If disease dynamics could be artificially slowed through active management (such as sanitation efforts to remove infected trees as has been done in beech bark disease [26] and Dutch elm disease [27]), then early production of basal sprouts could affect the initial dynamics of disease spread.

Over longer time scales, basal sprout production yields a larger host population and is necessary to maintain the host population when reproduction via seeds is unlikely. The efficacy of basal sprout production in either case decreases as secondary infection increases. When compared to no sprouting at all, basal sprouting with very high rates of secondary infection yields a similarly exhausted host population when seed production and germination are low but an even smaller host population when the seed production and germination are high. This suggests that basal sprouts should be considered even when reproduction via seeds is not fully limited by disease. Moreover, this suggests that management strategies that protect susceptible basal sprouts from secondary infection could sufficiently increase the host population to save the host from local extinction.

The dynamics of this mathematical model are consistent with time-series data of disease progression in redbay. Field work in redbay shows that vector populations exhibit great increase immediately after introduction and that both host and vector populations exhibit substantial decline over 2–5 years. In many locations, vector populations are maintained at very low levels for many years after the initial infestation, and in others no beetles were trapped in postepidemic plots [18,20,25]. It was hypothesized that vector

populations were being maintained through the use of small stems for brood production, despite their poor quality as host material. Our model supports this hypothesis because it yields an endemic equilibrium with positive host and vector populations, and those populations are very small under poor host growth and high basal sprout secondary infection. While our model does not predict extinction, it does allow for population levels so small that extinction is likely through stochastic events (e.g., increased vulnerability due to the small population paradigm [28]).

Time series data on disease progression in sassafras (outside of the range of redbay) is not available, but our results give a framework of what to expect in laurel wilt in sassafras stands. Sassafras does not respond to laurel wilt infection by producing basal sprouts, but sassafras has been known to produce epicormic shoots off the trunk or lower crown of the tree. These epicormic shoots can grow into branches and persist without infection symptoms for several years, despite infection in the main stem [20]. It is unclear how the production of epicormic shoots will affect disease dynamics. If matured epicormic shoots function as independent trees themselves, then our mathematical model suggests that a high rate of epicormic shoot production coupled with a low rate of secondary infection will maintain the population size. However, if the placement of epicormic shoots on decaying stems inhibits them from maturing into independent, tree-like stems, then our mathematical model suggests that epicormic shoot production is unlikely to preserve host populations from extinction. Further study of the function of epicormic shoots in sassafras trees infected with laurel wilt is merited.

The formulation and results of our model align to some degree with other ordinary differential equation models that do not specifically consider basal sprout production in vector-borne plant disease systems. Models of Dutch elm disease include host stage structure and dependence of the vector population on infected host material as does our model, but the models do not isolate basal sprout production [13]. Models of pine wilt disease have similar transmission terms as in our model, but many assume a constant influx of vector population independent of available material, which is inconsistent with redbay ambrosia beetle reproduction [8,9]. In the models for each of these diseases, vectors can be noncarriers of the pathogen. This assumption is also poor for laurel wilt due to the obligate nature of the vector-pathogen complex. Despite these differences, the dynamics of our model generally align with the dynamics of these aforementioned vector-borne disease models that predict either a stable disease-free equilibrium or a stable endemic equilibrium, depending on the size of the basic reproductive number. Our model also yields a stable endemic equilibrium but does not yield a disease-free equilibrium for a majority of the biologically feasible parameter space because a limit on host growth is not incorporated. A basic reproductive number thus was not calculated; however, we find that the endemic equilibrium is always stable, with trajectories never experiencing unbounded growth with or without disease.

Of course, there are disease systems to which this direct model does not apply. As a model for vector-borne tree disease, our model captures both the epidemiological impact of vector population size on disease progression and the ecological impact of disease progression on vector population size. Tree diseases transmitted without a vector are likely to have different dynamics and should be modeled differently. However, basal sprouts are also commonly produced in response to diseases with other modes of transmission, so similar questions are relevant and have been studied both empirically and with mathematical models.

In the case of airborne tree disease systems, the production of basal sprouts maintains the population despite high disease-induced mortality. For example, the fungal pathogen (*Cryphonectria parasitica*) that causes chestnut blight kills the main stem of American chestnut (*Castanea dentata*) and prevents seed production, but infected American Chestnuts can regenerate through the still-living root system [29]. Most sprouts of mature American Chestnuts are ripped out when the main stem falls, but the sprouts of infected saplings survive; thus, nearly all mature American Chestnut trees alive today in New England are

the matured sprouts of blight-infected saplings [29,30]. The tree disease sudden oak death is caused by an airborne, fungus-like pathogen (*Phytophthora ramorum*) and causes high mortality in mature coast live oak (*Quercus agrifolia*) and tanoak (*Notholithocarpus densiflorus*). Infected trees respond to infection by producing basal sprouts while root systems are still intact, and mathematical models suggest that this production will maintain the tree populations postepidemic [31] and impacts the efficacy of management strategies [32]. In the sense that basal sprouting in an airborne tree disease keeps the host population from extinction and that sprouting should be considered in the development of management strategies, our results are consistent with models of airborne diseases. However, we find the case of vector-borne diseases that basal sprouting can only maintain the population for small rates of basal sprout infection via secondary transmission.

All mathematical models include assumptions about population interactions that could affect model outputs. Most assumptions in our model are supported by empirical evidence, but at times sufficient empirical evidence is lacking to support one assumption over another. In particular, little is known specifically about how the beetle and infected host trees interact, so assumptions regarding this interaction had to be made. We have assumed that vectors are more strongly attracted to large stems than small stems (i.e.,  $\beta_P < \beta_M < \beta_L$ ). If this assumption were relaxed, we expect host mortality to be spread more evenly over stage classes rather than being highest for large trees. This could slow the speed of disease transmission because medium and small trees offer less volume of infected material for vector reproduction. We have also assumed that all equivalent infected volumes support equivalent vector reproduction. Although this is mathematically more tractable, in reality, galleries in small diameter stems produce smaller broods and have longer maturation times than galleries in large diameter stems [25]. As a result, our model could overestimate the utility of infected basal sprouts for vector reproduction and thus overestimate vector population at equilibrium. This could mean that the vector population could go locally extinct (as per the small population paradigm) if infected basal sprouts are of insufficient quality for substantial vector reproduction. Lastly, it is unclear how vector utilization of host material for reproduction contributes to the degradation of material. It is possible that this degradation is density independent (occurring to the same degree regardless of vector population size) or density dependent (with more degradation occurring when the vector population is large). With an absence of empirical evidence, we have assumed density-dependent degradation. An exploration of the consequences of this assumption is planned in future work.

## 5. Conclusions

We have created a mathematical model for the epidemiology of a lethal, vector-borne tree disease with host stage structure and basal sprout production by infected trees using laurel wilt as a model system. We assumed that all vectors carry the pathogen and that transmission could occur via contact with a vector or through direct contact between infected trees and their attached basal sprouts. We found that in vector-borne tree disease systems, the production of basal sprouts by an individual infected tree affects the disease dynamics on the population level. The disease remains endemic regardless of basal sprout production or secondary infection, but the host population is maintained at high levels only when basal sprout secondary infection is sufficiently infrequent when compared to basal sprout production. When basal sprout infection is high, the host population levels many years after initial introduction are the same or lower than in the absence of basal sprout production.

Basal sprout production and secondary infection can have profound effects on disease dynamics in trees. To include these effects in best practices for management and mitigation of a newly introduced vector-pathogen duplex, rapid experimentation to determine a number of factors related to basal sprouting will be critical. These, at least, include the rate of production of basal sprouts by infected trees, the rate of secondary infection of basal sprouts via root systems, and the nature of disease transmission, host association, and

vector biology. When these factors together reveal the potential reliance on basal sprout production for tree population persistence, management should potentially explore such interventions as active clearance of infected biomass, while otherwise strategies may be more effective when focusing on interruption of the spread of the vector. Models, such as the one here presented, provide a critical tool for proactive management as global spread of vectors and pathogens expose old forests to new threats.

**Author Contributions:** Conceptualization, K.R.B. and N.H.F.; data curation, K.R.B.; formal analysis, K.R.B.; funding acquisition, N.H.F.; investigation, K.R.B.; methodology, K.R.B.; project administration, K.R.B. and N.H.F.; resources, N.H.F.; software, K.R.B.; supervision, N.H.F.; validation, K.R.B. and N.H.F.; visualization, K.R.B.; writing—original draft, K.R.B. and N.H.F.; writing—review & editing, K.R.B. and N.H.F. All authors have read and agreed to the published version of the manuscript.

**Funding:** This research received no external funding.

**Institutional Review Board Statement:** Not applicable.

**Informed Consent Statement:** Not applicable.

**Data Availability Statement:** Not applicable.

**Acknowledgments:** We would like to thank Albert (Bud) Mayfield and KaDonna Randolph for their early guidance in understanding the biological system of laurel wilt and determining relevant questions for wildlife managers. We would also like to thank the organizers and participants of the Laurel Wilt Workshop: Disease Biology, Diagnosis, and Management, including Denita Hadziabdic, Romina Gazis, Pedro Pablo Parra, and Meher Ony, for sharing their insights on laurel wilt and other tree diseases that provided relevant context for confirming the structure of our mathematical model. Finally, we would like to thank Louis Gross, William E. Klingeman III and Olivia Prosper for their insightful comments and suggestions which greatly improved this manuscript.

**Conflicts of Interest:** The authors declare no conflict of interest.

## Appendix A. Calculation of Parameter Values

When possible, parameter values are estimated from the literature. Estimates on the diameter growth, survival, and volume of sassafras and other hardwoods is given in [33].

### Appendix A.1. Host Tree and Seed Mortality

Average size-based yearly survival probability for other hardwoods is 0.967 for saplings, 0.972–0.987 for medium trees, and 0.987–0.997 for large trees. Thus, we assume each year 1% of large trees die ( $\mu_L = 0.01$  trees/year), 2% of medium trees die ( $\mu_M = 0.02$  trees/year), and 3% of saplings die ( $\mu_P = 0.03$  trees/year). Redbay seeds remain viable for 1–2 years [17], and sassafras remain viable for 5–6 years [23]. We choose an intermediate viability of 3 years, and the yearly mortality rate is given by the reciprocal of the average lifespan ( $\mu_D = \frac{1}{3}$  seeds/year).

### Appendix A.2. Host Maturation

Size based maturation rates are calculated from data on the mean annual diameter growth by diameter class [33]. Within the category other hardwoods (data for sassafras not given individually), yearly growth rates corresponding to medium trees (2.5 cm–10 cm) vary between 0.11–0.98 cm/year. We choose a conservative annual diameter growth rate of 0.24 cm/year for medium trees. Accordingly, trees spend 31.25 years in this category ( $\frac{10\text{ cm} - 2.5\text{ cm}}{0.24\text{ cm/year}}$ ), which yields maturation rate of  $g_M = 1/(31.25\text{ years}) = 0.032$  trees/year. Data is unavailable for yearly diameter growth rate for stems under 2.5 cm. We assume a slightly smaller growth rate of 0.2 cm/year, which implies trees spend 12.5 years in the sapling category ( $\frac{2.5\text{ cm} - 0\text{ cm}}{0.2\text{ cm/year}}$  = 12.5 years). We then take the maturation rate to be the reciprocal of the time spent as a sapling (i.e.,  $g_P = 0.08$  trees/year). We assume that basal sprouts and saplings mature at the same rate (i.e.,  $g_B = g_P = 0.08$  trees/year).

### Appendix A.3. Seed Production and Germination

An estimate for the seed production rate was difficult to obtain from data. The mean yearly seed rain for sassafras is 0.0063 seeds/m<sup>2</sup>/year [34]. Assuming one tree spreads seeds over an area of 50 m<sup>2</sup> (arbitrarily selected), we have a per tree output of approximately  $r_L = 1/3$  seed per year. We assume medium trees have a slight reduction in seed production and take  $r_M = 0.9r_L$ . To an average reader, these quantities seem quite small. No data is available for seed germination rates in a forest setting. Accordingly, we select a seed germination rate of 10%, which yields a positive population growth rate in absence of disease. This rate seems quite high, perhaps in part because it is compensating for a small seed production rate.

### Appendix A.4. Tree Volume

Regarding the volume of trees, we assume that large trees provide twice as much suitable material as medium trees. Moreover, we assume medium trees provide twice as much suitable material as saplings and basal sprouts.

### Appendix A.5. Basal Sprout Parameters

In the absence of data to the contrary, we assume that basal sprouts and saplings mature at the same rate (i.e.,  $g_B = g_P = 0.08$  trees/year). Evans et al. [17] reported a very high redbay sprout mortality rate (79%) years after introduction of disease, but this statistic is not decoupled from mortality due to secondary infection. It is likely that most of the basal sprout mortality reported is due to secondary infection rather than naturally occurring mortality. We assume that natural (not disease-induced) mortality of basal sprouts is much lower than that of saplings because basal sprouts have the support of an existing root system. Thus, we take  $\mu_B = 0.0013$  trees/year.

In redbay plots, two-thirds of infected trees had at least one sprout 1.5 years after infection, and infected trees had on average 5 basal sprouts 7 years after infection [20]. Accordingly, rates for basal sprout production and infection were chosen to be on the magnitude of one basal sprout produced every six months to two years, and basal sprout infection was chosen on a similar magnitude.

## Appendix B. Equilibrium Analysis

We perform an equilibrium and stability analysis on Model (1). We do this by computing the Jacobian of Model (1), evaluating at the equilibrium, and determining the sign of the eigenvalues of the resulting matrix. If the eigenvalues all have negative real part, the equilibrium is called stable. Otherwise, the equilibrium is unstable. For more information, see [35,36].

We begin by determining equilibria. From the last differential equation equated to zero, we have that either  $X = 0$  or  $X = K$ , representing either extinction or maintenance of the vector population at equilibrium. We proceed with the former.

### Appendix B.1. Extinction of Vector Population

Equating all differential equations to zero and assuming  $X^* = 0$  immediately implies  $B_S^* = 0$  and that  $M_I^*$  is a negative multiple of  $L_I^*$  (assuming all positive parameters). Thus, the only biologically feasible equilibrium without vectors has  $B_S^* = M_I^* = L_I^* = 0$ . Furthermore, we obtain expressions for  $D^*$ ,  $P_S^*$ , and  $L_S^*$  as positive multiples of  $M_S^*$ . First, supposing  $M_S^* = 0$ , we yield an extinction equilibrium in which all susceptible host classes are zero. We have insufficient information to obtain representations for  $P_I^*$  or  $B_I^*$ . Any non-negative value of these would yield a biologically feasible extinction equilibrium. (That is, extinction of vectors despite unused infected material of small diameter remaining is possible.) The extinction equilibrium is given by  $(D^*, P_S^*, M_S^*, L_S^*, B_S^*, P_I^*, M_I^*, L_I^*, B_I^*, X^*)$ , they are given by  $Eq_0 = (0, 0, 0, 0, 0, P_I^*, 0, 0, B_I^*, 0)$ .

If  $M_S^*$  is nonzero at equilibrium (and thus other susceptible host classes are nonzero), we yield a nonextinction disease-free equilibrium when  $\gamma = \gamma_0 > 0$  where

$$\gamma_0 = \frac{\mu_D \mu_L (g_P + \mu_P)(g_M + \mu_M)}{g_P(g_M r_L + \mu_L r_M) - \mu_L(\mu_P + g_P)(\mu_M + g_M)}. \quad (\text{A1})$$

This threshold value  $\gamma_0$  is consistent with the minimum germination rate required for exponential growth (instead of exponential decay) of the host population in the absence of disease.

Due to the lack of restriction of the representations of  $P_I^*$  or  $B_I^*$ , we obtain a plane of possible equilibria (rather than a unique point). Thus, unused infected tree material could remain in the disease-free, nonextinction equilibrium. The disease-free, nonextinction equilibrium, expressed in the form  $(D^*, P_S^*, M_S^*, L_S^*, B_S^*, P_I^*, M_I^*, L_I^*, B_I^*, X^*)$ , is given by

$$\text{Eq}_1 = \left( \left( \frac{g_M r_L + \mu_L r_M}{(\gamma + \mu_D) \mu_L} \right) M_S^*, \left( \frac{g_M + \mu_M}{g_P} \right) M_S^*, M_S^*, \left( \frac{g_M}{\mu_L} \right) M_S^*, 0, P_I^*, 0, 0^*, B_I^*, 0 \right),$$

where  $M_S^*$  is positive and  $P_I^*$  and  $B_I^*$  are nonnegative.

We claim that under reasonable assumptions the disease-free, nonextinction equilibrium exists.

**Lemma A1.** Assume  $r_L > \mu_L$  and  $r_M > 3\mu_M$ . Furthermore, assume  $g_M < g_P$ ,  $\mu_M < \mu_P < g_P$ , and all parameters are positive. Then  $\gamma_0 > 0$ .

**Proof.** The numerator of Equation (A1) is always positive. Thus Equation (A1) is positive iff the denominator is positive. The denominator of Equation (A1) is positive iff

$$\frac{r_L}{\mu_L} > 1 + \frac{\mu_M g_P + \mu_M \mu_P + g_M \mu_P - r_M g_P}{g_M g_P}.$$

By assumption,  $\frac{\mu_P}{g_P} < 1$ ,  $\frac{g_M}{g_P} < 1$ , and  $\frac{\mu_P}{\mu_M} < 1$ . Thus,

$$1 + \frac{\mu_P}{g_P} + \frac{g_M}{g_P} \frac{\mu_P}{\mu_M} < 3.$$

Multiplying by  $\mu_M$  and applying the lower bound of  $r_M$  yields

$$\mu_M \left( 1 + \frac{\mu_P}{g_P} + \frac{g_M}{g_P} \frac{\mu_P}{\mu_M} \right) < 3\mu_M < r_M.$$

This inequality is equivalent to

$$\mu_M g_P + \mu_M \mu_P + g_M \mu_P < r_M g_P.$$

Consequently,

$$\frac{\mu_M g_P + \mu_M \mu_P + g_M \mu_P - r_M g_P}{g_M g_P} < 0,$$

and

$$1 + \frac{\mu_M g_P + \mu_M \mu_P + g_M \mu_P - r_M g_P}{g_M g_P} < 1 < \frac{r_M}{\mu_L}.$$

This is sufficient to show  $\gamma$  in Equation (A1) is positive.  $\square$

The assumptions in Lemma A1 are reasonable under normal biological conditions. Adult trees produce a large quantity of seeds and suffer mortality infrequently. Thus, the lower bounds on the reproductive output of medium and large trees hold throughout the biologically feasible parameter space. Regarding the growth rates of medium trees

and saplings, we note that the medium class represents a larger spread of diameters than saplings (stems less than 2.5 cm DBH). As such, a tree that grows in DBH linearly will spend more time in the medium size class than in the sapling class. Thus,  $g_M < g_P$ . However, medium trees are more resilient than saplings and, as such, have a lower mortality rate, i.e.,  $\mu_M < \mu_P$ . Finally, the assumption that  $g_P > \mu_P$  requires that more saplings mature than die in a given time step. We maintain these inequalities throughout the swept parameter space.

Because the assumptions of Lemma A1 hold over the biologically feasible parameter space, we conclude the boundary representation for  $\gamma$  is positive throughout the biological feasible parameter space. Moreover, numerical experiments show that the value of  $\gamma$  when evaluated at parameters within the biologically feasible parameter space is of an order of magnitude that is also biologically feasible. Thus, we have, mathematically, a biologically feasible disease-free equilibrium with a viable host population. However, this boundary case is unlikely to persist through natural perturbations of parameter values.

To determine the stability of these equilibria, we compute the Jacobian of the ODE system and substitute  $A = 0$ . The characteristic polynomial of the Jacobian contains no other state variables, so we proceed with stability of both equilibria that exclude vectors simultaneously. The characteristic polynomial in  $x$  of the Jacobian of the system at an equilibrium with no vectors is a tenth-degree polynomial, which can be factored as

$$x^4(\omega - x)(g_B + \mu_b + \sigma + x)p(x),$$

where  $p(x)$  is a fourth-degree polynomial in  $x$ . Thus,  $\omega$ ,  $-(g_B + \mu_b + \sigma)$ , and 0 are eigenvalues. Because  $\omega$  is assumed positive, both equilibria are unstable, despite the zero eigenvalues.

#### Appendix B.2. Endemic Disease Equilibrium

If  $X \neq 0$ , then  $X = K$ , where  $K$  is a function of the infected classes. That is,  $X = \frac{B_I + L_I + M_I + P_I}{v_0}$ . We immediately obtain the expressions

$$\begin{aligned} P_I^* &= \frac{P_S \beta_P v_P}{\delta_P}, \\ M_I^* &= \frac{M_S \beta_M v_M}{\delta_M}, \text{ and} \\ L_I^* &= \frac{L_S \beta_L v_L}{\delta_L}. \end{aligned}$$

We proceed with the remaining differential equations, setting one equal to zero, solving for a variable, and substituting that expression into the other equations, yielding

$$\begin{aligned} B_S^* &= \frac{B_I \delta_B X}{\sigma v_B}, \\ P_S^* &= \frac{\delta_P \left( M_S g_M v_0 - L_S v_0 \mu_I - L_S \beta_L \left( A - \frac{P_I}{v_0} \right) \right)}{L_S \beta_L \beta_P v_P}, \\ B_I &= \frac{\sigma v_0 v_B \left( \frac{L_S \beta_L \rho_L}{\delta_L} + \frac{M_S \beta_M \rho_M}{\delta_M} \right)}{\delta_B \left( L_I + M_I - \frac{v_0 \left( L_S \mu_L - M_S g_M + \frac{L_S \beta_L (L_I + M_I)}{v_0} \right)}{L_S \beta_L} \right) (g_B + \mu_B + \sigma)}, \end{aligned}$$

and

$$M_S^* = \frac{D (\gamma + \mu_D) - L_S r_L}{r_M}.$$

Doing so increases the degree of the remaining equations to be solved and the process ultimately fails when two variables remain,  $L_s$  and  $D$ , and two differential equations,  $\frac{dP_s}{dt}$  and  $\frac{dM_s}{dt}$ . Each differential equation can be expressed in factored form as

$$\frac{dP_s}{dt} = \frac{a(D, L_s)}{L_s^2 c(D, L_s)} \text{ and} \quad (\text{A2})$$

$$\frac{dM_s}{dt} = \frac{b(D, L_s)}{L_s c(D, L_s)} \quad (\text{A3})$$

where  $a(D, L_s)$  is a third-degree polynomial in  $D$  and a fourth-degree polynomial in  $L_s$  and  $b(D, L_s)$  is a third-degree polynomial in both variables. Neither differential equation can be solved for either remaining variable using symbolic algebra in MATLAB.

Despite not having expressions for  $D^*$  and  $L_s^*$ , we proceed in search of support that an endemic equilibrium exists. We see that we have an endemic equilibrium iff there exists a pair  $(D^*, L_s^*)$  such that  $a(D^*, L_s^*) = b(D^*, L_s^*) = 0$ . These equations cannot be solved explicitly for either remaining state variable. However, it can be shown (using an intermediate value theorem argument) that  $a(D, L_s)$  and  $b(D, L_s)$  each must have a nonempty set of positive roots. Moreover, in a sweep of the biologically feasible parameter space, we demonstrate that the curves of solutions to each equation always intersect.

Numerical investigations suggest that there exists a pair  $(D^*, L_s^*)$  such that  $a(D^*, L_s^*) = b(D^*, L_s^*) = 0$  throughout the biologically feasible parameter space. We use Latin hypercube sampling with  $N = 1000$  samples varying  $r_L, \gamma, g_p, \mu_D, \mu_L, \mu_B, \beta_L, \rho, \sigma, \delta_P$ , and  $\omega$  between  $10^{-2}\alpha$  and  $10^2\alpha$  where  $\alpha$  is the default value listed in Table 1. Parameters that depend on the varied parameters were covaried. To ensure that the sampled parameter space is biologically feasible, we remove samples in which  $\gamma > \gamma_0 > 0$  does not hold. This removes, on average, approximately 25% of samples. Parameter combinations that were removed generally had relatively small values for  $r_L, \gamma$ , and  $g_p$  (parameters that positively affect host growth) and/or relatively large values for  $\mu_D, \mu_L$ , and  $\mu_B$  (parameters that negatively affect host growth). In case this removal left regions of parameter space insufficiently sampled, we perform a second sweep that restricts  $r_L, \gamma$ , and  $g_p$  to  $10^{-2}\alpha$  and  $10^1\alpha$  and  $\mu_D, \mu_L$ , and  $\mu_B$  to  $10^{-1}\alpha$  and  $10^2\alpha$ , where  $\alpha$  is the default value listed in Table 1. We sample with  $N = 10,000$  and again remove samples in which  $\gamma > \gamma_0 > 0$  does not hold (approximately 95% of samples).

To find the pair  $(D^*, L_s^*)$  for each parameter combination, we discretize the set of positive roots  $\{(L_s, D^a)\}$  to  $a(D, L_s)$  and  $\{(L_s, D^b)\}$  to  $b(D, L_s)$  by evaluating each expression at values of  $L_s$  and approximating the values of  $D_a$  and  $D_b$  using the function `solve`. We inspect the discretized set of roots to each equation and search for an intersection of the curves in the form of a sign change in the expression  $D^a - D^b$  at values of  $D^a$  and  $D^b$  that are positive and real. A positive, real pair  $(D^*, L_s^*)$  was located at every combination in each sweep. Thus, there appears to always be a pair of positive values for the seed population and the large susceptible tree population that are roots of both  $a(D, L_s)$  and  $b(D, L_s)$ . By using these approximations of  $D^*$  and  $L_s^*$ , we can approximate the values of all states at the endemic equilibrium using the algebraic expressions above. For example, the endemic equilibrium at the default parameter values is given by  $(D^*, P_S^*, M_S^*, L_S^*, B_S^*, P_I^*, M_I^*, L_I^*, B_I^*, X^*) = (0.5438, 0.4805, 0.7056, 0.0719, 0.6889, 0.0072, 0.5292, 0.4315, 3.2595, 12.6864)$ . We conclude that numerical experiments support the existence of an endemic equilibrium throughout the biologically feasible parameter space.

#### Appendix B.3. Numerical Support of Stability of Endemic Equilibrium

To determine the stability of the equilibrium, we investigate the eigenvalues of the Jacobian of the system evaluated at the endemic equilibrium. The eigenvalues of this  $10 \times 10$  system cannot be computed algebraically. Thus, we resort to numerical experiments. For each parameter combination in the sweeps, we evaluate the Jacobian of the system at both the parameter values and at the approximations of the state variables at the endemic

equilibrium computed previously. We compute the eigenvalues of the resulting matrix. Throughout the biologically feasible parameter space, the eigenvalues of the Jacobian have negative real part. We conclude that numerical experiments support the asymptotic stability of the endemic equilibrium throughout the biologically feasible parameter space.

#### Appendix B.4. Numerical Support of Global Stability

To determine the global stability of the endemic equilibrium, we confirm that numerical approximations of the solutions to the ODE system (computed via the MATLAB function `ode45`) converge to the theoretical endemic equilibrium. For each parameter combination, we approximate the value of  $D^\infty$  and  $L_S^\infty$  by running the model for 10,000 years or until equilibrium is reached and note the number of seeds and large trees. We compare the approximations of  $(D^*, L_S^*)$  against the values of  $(D^\infty, L_S^\infty)$ . The Euclidean difference between these two points can be made less than  $10^{-2}$  trees throughout the vast majority of the biologically feasible parameter space by using an increasingly fine mesh to compute  $D^*$  and  $L_S^*$ . (This is not the case when host life-cycle parameters are restricted and when  $\beta$  is less than 1% of the default value. In this case, solutions the pairs  $(D^*, L_S^*)$  and  $(D^\infty, L_S^\infty)$  can be distant, but both pairs are sufficiently far from the origin. We blame the inconsistency on numerical error within `ode45`, `solve`, or both for exceptionally small values of  $\beta$ .)

We also evaluate  $|a(D^\infty, L_S^\infty)|$  and  $|b(D^\infty, L_S^\infty)|$  and confirm the values are near zero to confirm the system is at equilibrium, which would suggest the equilibrium reached is the endemic equilibrium. The results are always less than  $10^{-19}$  and do not vary with the size of the sampled parameter space or number of parameter combinations considered. This is numerical support of the global stability of the endemic equilibrium throughout the biologically feasible parameter space.

## References

1. Aukema, J.E.; McCullough, D.G.; Von Holle, B.; Liebhold, A.M.; Britton, K.; Frankel, S.J. Historical accumulation of nonindigenous forest pests in the continental United States. *BioScience* **2010**, *60*, 886–897. [[CrossRef](#)]
2. Pimentel, D.; Zuniga, R.; Morrison, D. Update on the environmental and economic costs associated with alien-invasive species in the United States. *Ecol. Econ.* **2005**, *52*, 273–288. [[CrossRef](#)]
3. Del Tredici, P. Sprouting in temperate trees: A morphological and ecological review. *Bot. Rev.* **2001**, *67*, 121–140. [[CrossRef](#)]
4. Paciorek, C.J.; Condit, R.; Hubbell, S.P.; Foster, R.B. The demographics of resprouting in tree and shrub species of a moist tropical forest. *J. Ecol.* **2000**, *88*, 765–777. [[CrossRef](#)]
5. Bond, W.J.; Midgley, J.J. Ecology of sprouting in woody plants: The persistence niche. *Trends Ecol. Evol.* **2001**, *16*, 45–51. [[CrossRef](#)]
6. Carr, D.E.; Banas, L.E. Dogwood anthracnose (*Discula destructiva*): Effects of and consequences for host (*Cornus florida*) demography. *Am. Midl. Nat.* **2000**, *143*, 169–177. [[CrossRef](#)]
7. Mamiya, Y. Pathology of the pine wilt disease caused by *Bursaphelenchus xylophilus*. *Annu. Rev. Phytopathol.* **1983**, *21*, 201–220. [[CrossRef](#)]
8. Shi, R.; Zhao, H.; Tang, S. Global dynamic analysis of a vector-borne plant disease model. *Adv. Differ. Equ.* **2014**, *2014*, 59. [[CrossRef](#)]
9. Lee, K.S.; Kim, D. Global dynamics of a pine wilt disease transmission model with nonlinear incidence rates. *Appl. Math. Model.* **2013**, *37*, 4561–4569. [[CrossRef](#)]
10. Collin, E.; Bilger, I.; Eriksson, G.; Turok, J. The conservation of elm genetic resources in Europe. In *The Elms*; Springer: Berlin/Heildeberg, Germany, 2000; pp. 281–293.
11. Peterken, G.; Mountford, E. Long-term change in an unmanaged population of wych elm subjected to Dutch elm disease. *J. Ecol.* **1998**, *86*, 205–218. [[CrossRef](#)]
12. Gibbs, J. Development of the Dutch elm disease epidemic in southern England, 1971–6. *Ann. Appl. Biol.* **1978**, *88*, 219–228. [[CrossRef](#)]
13. Swinton, J.; Gilligan, C.A. Dutch elm disease and the future of the elm in the UK: A quantitative analysis. *Philos. Trans. R. Soc. Lond. Ser. Biol. Sci.* **1996**, *351*, 605–615.
14. Swinton, J.; Gilligan, C.A. A Modelling Approach to the Epidemiology of Dutch Elm Disease. In *A Modelling Approach to the Epidemiology of Dutch Elm Disease*; Springer: Boston, MA, USA, 2000; pp. 73–101.
15. Fraedrich, S.; Harrington, T.; Rabaglia, R.; Ulyshen, M.; Mayfield Iii, A.; Hanula, J.; Eickwort, J.; Miller, D. A fungal symbiont of the redbay ambrosia beetle causes a lethal wilt in redbay and other Lauraceae in the southeastern United States. *Plant Dis.* **2008**, *92*, 215–224. [[CrossRef](#)]
16. Ploetz, R.; Kendra, P.; Choudhury, R.; Rollins, J.; Campbell, A.; Garrett, K.; Hughes, M.; Dreaden, T. Laurel wilt in natural and agricultural ecosystems: Understanding the drivers and scales of complex pathosystems. *Forests* **2017**, *8*, 48. [[CrossRef](#)]

17. Evans, J.P.; Scheffers, B.R.; Hess, M. Effect of laurel wilt invasion on redbay populations in a maritime forest community. *Biol. Invasions* **2014**, *16*, 1581–1588. [[CrossRef](#)]
18. Hanula, J.L.; Mayfield, A.E., III; Fraedrich, S.W.; Rabaglia, R.J. Biology and host associations of redbay ambrosia beetle (Coleoptera: Curculionidae: Scolytinae), exotic vector of laurel wilt killing redbay trees in the southeastern United States. *J. Econ. Entomol.* **2008**, *101*, 1276–1286. [[CrossRef](#)]
19. Randolph, K.C. Status of *Sassafras albidum* (Nutt.) Nees in the Presence of Laurel Wilt Disease and Throughout the Eastern United States. *Southeast. Nat.* **2017**, *16*, 37–58. [[CrossRef](#)]
20. Cameron, R.S.; Hanula, J.; Fraedrich, S.; Bates, C. Progression and impact of laurel wilt disease within redbay and sassafras populations in southeast Georgia. *Southeast. Nat.* **2015**, *14*, 650–674. [[CrossRef](#)]
21. Formby, J.P.; Rodgers, J.C.; Koch, F.H.; Krishnan, N.; Duerr, D.A.; Riggins, J.J. Cold tolerance and invasive potential of the redbay ambrosia beetle (*Xyleborus glabratus*) in the eastern United States. *Biol. Invasions* **2018**, *20*, 995–1007. [[CrossRef](#)]
22. Gilligan, C.A. Sustainable agriculture and plant diseases: An epidemiological perspective. *Philos. Trans. R. Soc. Biol. Sci.* **2008**, *363*, 741–759. [[CrossRef](#)]
23. Meadows, J.S.; Bonner, F.T.; Haywood, J.D. Soil-seed bank survival in forests of the Southern United States. *New For.* **2006**, *32*, 335–345. [[CrossRef](#)]
24. Potter, C.; Harwood, T.; Knight, J.; Tomlinson, I. Learning from history, predicting the future: The UK Dutch elm disease outbreak in relation to contemporary tree disease threats. *Philos. Trans. R. Soc. Biol. Sci.* **2011**, *366*, 1966–1974. [[CrossRef](#)] [[PubMed](#)]
25. Maner, M.L.; Hanula, J.L.; Horn, S. Population trends of the redbay ambrosia beetle (Coleoptera: Curculionidae: Scolytinae): Does utilization of small diameter redbay trees allow populations to persist? *Fla. Entomol.* **2014**, *97*, 208–217. [[CrossRef](#)]
26. Heyd, R.L. Managing beech bark disease in Michigan. In *Beech Bark Disease: Proceedings of the Beech Bark Disease Symposium*; General Technical Report (GTR) NE-331; Evans, C.A., Lucas, J.A., Twery, M.J., Eds.; US Department of Agriculture Forest Service, Northern Research Station: Washington, DC, USA, 2005; pp. 128–132.
27. Scheffer, R.; Voeten, J.; Guries, R. Biological control of Dutch elm disease. *Plant Dis.* **2008**, *92*, 192–200. [[CrossRef](#)] [[PubMed](#)]
28. Caughley, G. Directions in conservation biology. *J. Anim. Ecol.* **1994**, *63*, 215–244. [[CrossRef](#)]
29. Paillet, F.L. Chestnut: History and ecology of a transformed species. *J. Biogeogr.* **2002**, *29*, 1517–1530. [[CrossRef](#)]
30. Paillet, F.L. Growth-form and ecology of American chestnut sprout clones in northeastern Massachusetts. *Bull. Torrey Bot. Club* **1984**, *3*, 316–328. [[CrossRef](#)]
31. Cobb, R.C.; Filipe, J.A.; Meentemeyer, R.K.; Gilligan, C.A.; Rizzo, D.M. Ecosystem transformation by emerging infectious disease: Loss of large tanoak from California forests. *J. Ecol.* **2012**, *100*, 712–722. [[CrossRef](#)]
32. Filipe, J.A.; Cobb, R.C.; Salmon, M.; Gilligan, C.A. Management strategies for conservation of tanoak in California forests threatened by sudden oak death: A disease-community feedback modelling approach. *Forests* **2019**, *10*, 1103. [[CrossRef](#)]
33. Smith, W.B. *Diameter Growth, Survival, and Volume Estimates for Trees in Indiana and Illinois*; US Department of Agriculture, Forest Service, North Central Forest: Washington, DC, USA, 1984; Volume 257
34. Clark, J.S.; Lavine, M. Implications of Seed Banking for Recruitment of Southern Appalachian Woody Species. *Ecology* **2005**, *86*, 85–95.
35. Strogatz, S.H. *Nonlinear Dynamics and Chaos: With Applications to Physics, Biology, Chemistry, and Engineering*; CRC Press: Boca Raton, FL, USA, 2018.
36. Brauer, F.; Castillo-Chavez, C.; Castillo-Chavez, C. *Mathematical Models in Population Biology and Epidemiology*; Springer: Berlin/Heildeberg, Germany, 2012; Volume 2.

**Disclaimer/Publisher's Note:** The statements, opinions and data contained in all publications are solely those of the individual author(s) and contributor(s) and not of MDPI and/or the editor(s). MDPI and/or the editor(s) disclaim responsibility for any injury to people or property resulting from any ideas, methods, instructions or products referred to in the content.